A Comparative Study on Electrical Characteristics of Crystalline AlN Thin Films Deposited by ICP and HCPA-Sourced Atomic Layer Deposition

Altuntas, H.; Bayrak, T.;

Originally published:

December 2016

Electronic Materials Letters 13(2017)2, 114-119

DOI: https://doi.org/10.1007/s13391-017-6111-z

Electron. Mater. Lett.
DOI: 10.1007/s13391-017-6111-z

A Comparative Study on Electrical Characteristics of Crystalline AlN Thin Films Deposited by ICP and HCPA-Sourced Atomic Layer Deposition

Halit Altuntas[1,*] and Turkan Bayrak[2,3,4]

[1]Faculty of Science, Department of Physics, Cankiri Karatekin University, Cankiri 18100, Turkey
[2]Helmholtz-Zentrum Dresden-Rossendorf, Bautzner Landstrabe 400, Dresden 01328, Germany
[3]Technische Universität Dresden, cfaed, Dresden 01062, Germany

(received date: 13 April 2016 / accepted date: 14 November 2016)

In this work, we aimed to investigate the effects of two different plasma sources on the electrical properties of low-temperature plasma-assisted atomic layer deposited (PA-ALD) AlN thin films. To compare the electrical properties, 50 nm thick AlN films were grown on *p*-type Si substrates at 200 °C by using an inductively coupled RF-plasma (ICP) and a stainless steel hollow cathode plasma-assisted (HCPA) ALD systems. Al/AlN/*p*-Si metal-insulator-semiconductor (MIS) capacitor devices were fabricated and capacitance versus voltage (*C-V*) and current-voltage (*I-V*) measurements performed to assess the basic important electrical parameters such as dielectric constant, effective charge density, flat-band voltage, breakdown field, and threshold voltage. In addition, structural properties of the films were presented and compared. The results show that although HCPA-ALD deposited AlN thin films has structurally better and has a lower effective charge density (N_{eff}) value than ICP-ALD deposited AlN films, those films have large leakage current, low dielectric constant, and low breakdown field. This situation was attributed to the involvement of Si atoms into the AlN layers during the HCPA-ALD processing leads to additional current path at AlN/Si interface and might impair the electrical properties.
PACS: 73.30.+y: 73.40.Qv: 73.40.Ns

Keywords: aluminum nitride, effective charge density, atomic layer deposition (ALD), hollow-cathode plasma, inductively coupled RF-plasma, dielectric

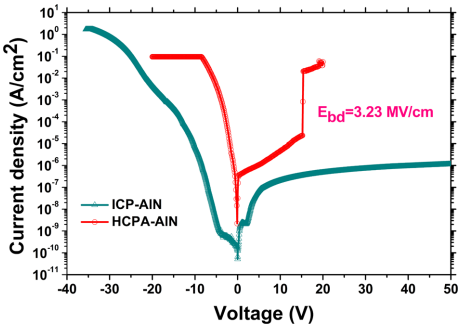

1. INTRODUCTION

AlN, GaN, InN and their alloys are called group III-Nitrides and the unique properties of the group III-Nitrides make them attractive materials for optoelectronics and microelectronics devices. Aluminum nitride (AlN) has the widest direct band gap (6.2 eV) in all group III-Nitrides. Also, it has good piezoelectric properties, high thermal conductivity, good thermal and chemical stability, large resistivity, and low toxicity.[1-7] Especially, due to AlN has a higher dielectric constant compared to SiO_2 and Si_3N_4, the potential of AlN as an alternative gate dielectric material is important.[8-11] Depending on the applications, AlN thin films have been deposited using a variety of techniques, the main techniques being metal-organic chemical vapor deposition (MOCVD)[12] and molecular beam epitaxy (MBE).[13] But these techniques require substrate temperatures which typically are above 1000 °C and this temperature is not suitable for post-processing on Si substrates used in CMOS technology. Therefore, low-temperature growth methods have to be used for this reason.

As an alternative to high temperature deposition methods, atomic layer deposition (ALD) which is a special type of chemical vapor deposition (CVD) technique, has been developed recently to deposit thin films at low substrate

*Corresponding author: altunhalit@gmail.com

temperatures (typically below 300 °C).[14,15] This method is based on self-terminating surface reactions which means the precursor (gaseous reactants) do not tend to react with themselves and gas-solid reaction terminates when all of the available surface sites are bonding. This growth mechanism is called as "self-limiting" and the most important feature of ALD technique. This key feature provides excellent thickness control at sub-nanometer scale and uniform and conformal film coatings at low substrate temperatures. In addition, to achieve lower deposition temperature, reactivity of the precursors can be enhanced by external energy source such as plasma. Thus, plasma source creates highly reactive radicals that contribute to chemical reactions occurring at the surface which enables to further lower the growth temperatures compared to conventional thermal ALD reactions. Our group has reported some studies on the current transport mechanisms in AlN thin films deposited by an inductively coupled plasma (ICP) source assembled PEALD system.[16,17] However, using the quartz-based ICP source led to relatively high oxygen impurities in III-nitride thin films and therefore, ICP source was replaced with a stainless-steel capacitively-coupled hollow cathode plasma (HCP) source. In this study, we reported that basic electrical parameters of AlN thin films grown at low temperatures by using hollow-cathode plasma-assisted atomic layer deposition (HCPA-ALD) and compared the AlN thin films deposited by ICP-sourced ALD system to understand how effects of different plasma sources on the electrical properties.

2. EXPERIMENTAL PROCEDURE

AlN thin films with thicknesses ~50 nm were deposited on solvent-cleaned *p*-type Si substrates. Before deposition, the native oxide layers of the Si substrates were removed with piranha solution. After cleaning process, ~80 nm thick Al ohmic contact was formed on the back side of the substrates by thermal evaporation and subsequent rapid thermal annealing at 450 °C for 2 min under 100 sccm N_2 flow while the top wafer side was protected with a layer of photoresist. Si(100) substrates with back ohmic contacts were then loaded into a customized Fiji F200-LL ALD reactor (Ultratech/CambridgeNanotech Inc.) equipped with a capacitively-coupled hollow-cathode plasma source (Meaglow Inc.). All depositions started with the metalorganic pulse. Trimethylaluminum ($AlMe_3$) and N_2/H_2 plasma were used as the Al and N precursors, respectively. $AlMe_3$ was kept at room temperature and 5N-grade N_2 and H_2 plasma gases along with the carrier gas, Ar, were further purified using MicroTorr gas purifiers. Metalorganic precursor pulses and plasma gases were carried from separate lines by 30 and 100 sccm Ar, respectively. The speed of the Adixen ATH 400 M turbo pump was adjusted in order to keep the reactor base pressure around ~150 mTorr during the growth experiment. Remote RF-plasma (300 W) was activated at each cycle only during the flow of N-containing plasma gas. Unless stated otherwise, the system was purged for 10 s after each exposure. All growth experiments were carried out at a fixed substrate temperature of 200 °C. On the other hand AlN thin films with thicknesses ~50 nm were deposited on the same *p*-type Si substrates at 200 °C by using ICP-sourced ALD system, where one PEALD cycle consisted of: 0.1 s $AlMe_3$ pulse/10 s Ar purge/40 s, 50 sccm, 300W NH_3 plasma/10 s Ar purge. During the deposition, $AlMe_3$ and NH_3 were carried from separate lines using 60 and 200 sccm Ar, respectively.

Top contacts of the metal-insulator-semicondcutor (MIS) structures were formed by another thermal evaporation (~80 nm thick Al) process followed with lift-off for both ICP and HCPA-ALD deposited AlN films. MIS capacitor structures with AlN as the insulating layer were fabricated on 25 mm × 40 mm *p*-type Si(100) substrates using class 100 and 1000 cleanroom facilities. Al and AlN layers were patterned simultaneously to obtain MIS devices with 105,225 and 59,300 μm^2 active areas for HCPA-ALD and ICP-ALD deposited films, respectively. For the development of AZ 5214E photoresist, AZ 400K developer (MicroChemicals GmbH) (AZ 400K:H_2O = 1:4) was used.

Capacitance-voltage (*C-V*) and current-voltage (*I-V*) characteristics of the fabricated MIS capacitor structures were measured under dark using a semiconductor parameter analyzer (Keithley 4200-SCS), which is connected to a DC probe station (Cascade Microtech PM-5). *C-V* curves were obtained in the frequency of 1 MHz. The structural properties of HCPA-ALD and ICP-ALD grown AlN films were characterized via grazing incidence X-ray diffraction (GIXRD). GIXRD measurements were performed in a PANalytical X'Pert PRO MRD diffractometer using Cu Kα radiation. Ellipsometric spectra of the films were recorded in the wavelength range of 300-850 nm at three angles of incidence using a variable angle spectroscopic ellipsometer (J.A. Woollam). Optical constants were modeled by the Cauchy dispersion function and Tauc-Lorentz (TL) function, and used for the estimation of the film thicknesses. Surface morphologies of HCPA and ICP-sourced ALD deposited AlN thin films were investigated using atomic force microscopes (AFM, Asylum Research MFP-3D) latter operating in the tapping mode using a triangular tip.

3. RESULTS AND DISCUSSION

3.1 Grazing incidence X-ray diffraction and AFM measurements

GIXRD patterns of HCPA-ALD and ICP-ALD deposited AlN thin films with ~50 nm thickness on Si (100) substrates are presented in Fig. 1. All labeled Bragg diffraction peaks on the patterns were reflections of the hexagonal wurtzite

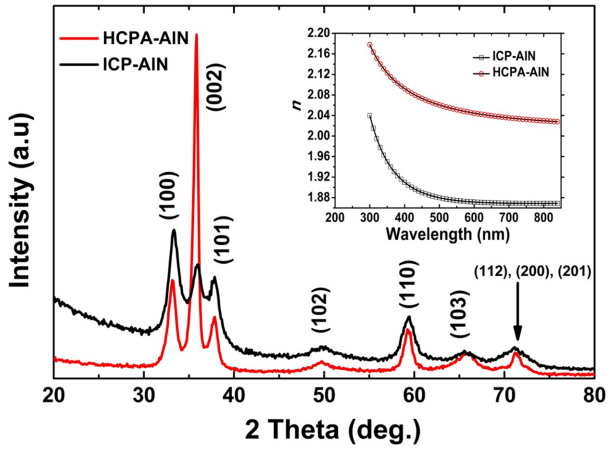

Fig. 1. GIXRD patterns of ~50 nm thick AlN thin film deposited using ICP and HCP-sourced ALD systems. Films are polycrystalline with a hexagonal wurtzite structure. Inset shows the spectral refractive indexes (*n*) of the deposited AlN thin films.

phase and positions of those peaks perfectly matching with the literature (ICDD reference code: 00-025-1133).

As can be seen in Fig. 1, due to (002) reflections in HCPA-ALD deposited AlN thin films have higher intensity and narrower peak than ICP-ALD deposited AlN thin films, crystallite size values are larger, and therefore it means an enhancement in the crystalline quality for the HCPA-ALD deposited AlN thin films. This GIXRD patterns reveal that AlN thin films can be deposited successfully by using HCP-ALD technique at low temperature.

On the other hand, the refractive indexes (*n*) of the ICP and HCPA-sourced ALD deposited AlN thin film were measured within the wavelength range of 300-850 nm by spectroscopic ellipsometry. As known, *n* value depends on film crystallinity; the *n* values that were reported in the literature for polycrystalline AlN films[18] are in good agreement with the present data, which again confirms the polycrystalline nature of the deposited films. The optical dielectric constant (κ_{op}) is equal to the square of the refractive index, which was already obtained by spectroscopic ellipsometry (i.e., $\kappa_{op} = n^2$). The *n* values were measured to be 1.87 and 2.04 at 633 nm, resulting in a κ_{op} of 3.49 and 4.16 for ICP and HCPA-sourced ALD deposited AlN thin films, respectively. As described in our group' previous reports, by using the hollow-cathode plasma, significant fraction of oxygen impurities segregate at the grain boundaries, the increase in crystallite size might indicate a decrease in the O impurity concentration.[19]

The 3D-surface morphologies of ~50 nm thick HCPA and ICP-sourced ALD deposited AlN thin films are given in Fig. 2(a) and (b) and root-mean-square (rms) roughnesses of the films were measured as 0.721 and 0.678 nm from 2 μm × 2 μm scan areas, respectively. The rms value of HCPA-sourced ALD deposited AlN thin films is a little bit higher and therefore has a poorer surface compared to ICP-sourced ALD deposited AlN films.

3.2 Electrical (C-V and I-V) characteristics

To assess the basic electrical characteristics of the HCPA and ICP-sourced ALD deposited AlN thin films, room temperature capacitance versus voltage (*C-V*) measurements were performed at a frequency of 1 MHz and given in Fig. 3.

At large negative gate voltage region, the capacitance of the dielectric films is dominant in the total capacitance, indicating accumulation. The dc gate bias voltage is swept from negative voltage to positive voltage and returns to initial value to check hysteresis behavior. In ideal case, there should be no hysteresis with sweep direction and the flat-band voltage should be near 0 V, and the fact that a remarkable hysteresis curve is observed in Fig. 3. indicates the presence of trapped charge at the interface and mobile charges in the AlN films. On the other hand, as can be seen in Fig. 3, the flat-band voltage has a negative shift which may be caused by immobile positive charges located in the bulk AlN dielectric film and interface between the AlN film-silicon substrate.

In strong accumulation region, using the maximum

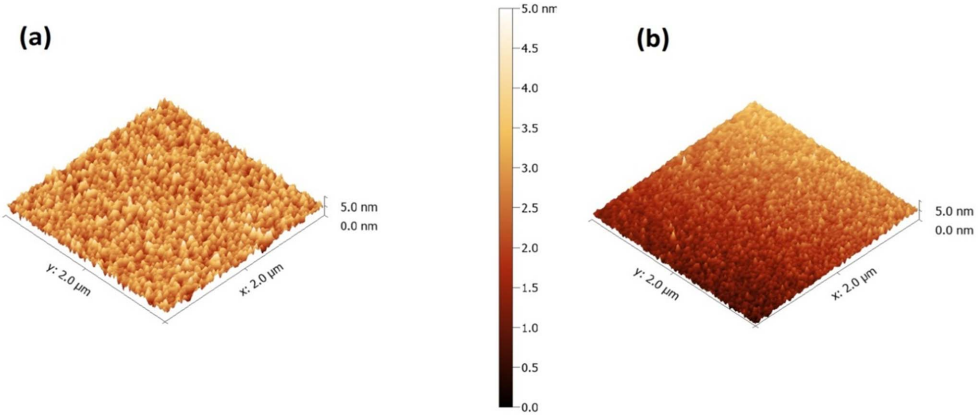

Fig. 2. 3D-surface morphologies of ~50 nm thick AlN thin film deposited using HCPA (a) and ICP-sourced (b) ALD systems.

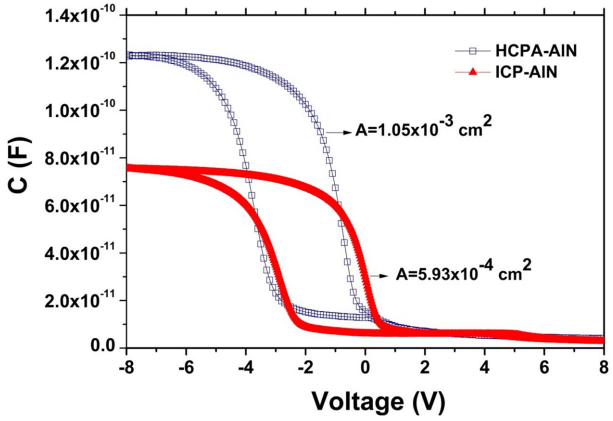

Fig. 3. Typical 1 MHz *C-V* hysteresis under bi-direction gate bias scan for AlN thin film deposited using HCPA and ICP-sourced ALD systems.

capacitance of the films, C_i, the dielectric constant of the films (ε_d) can be calculated from $C_i = \varepsilon_d \varepsilon_0 A/t_d$, where A is the area of the MIS capacitor, ε_0 is the permittivity of free space, and t_d is the thickness of the AlN film. Using this formula, the dielectric constants were calculated as 6.6 and 7.1 for HCPA and ICP-sourced ALD deposited AlN films, respectively, and those values are similar with reported studies.[20,21]

The effective charges depending on their type shift the *C-V* curve to either left or right. The effective charge density (N_{eff}) can be calculated based on the following equation:

$$N_{eff} = \frac{C_i(\phi_{ms} - V_{FB})}{qA} \quad (1)$$

where, ϕ_{ms} is the difference between metal (Al) and semiconductor (Si) work functions, q is the electronic charge, V_{FB} is the flat-band voltage, and A is the area of the capacitor. In order to determine V_{FB}, flat-band capacitance (C_{FB}) method can be used. The *p*-type Si surface at the flat-band condition is given by,

$$C_{FBS} = \frac{\varepsilon_{Si}\varepsilon_0}{\lambda} \quad (2)$$

where, ε_{Si} is the dielectric constant of Si (i.e., 11.8) and λ is the Debye length of *p*-type Si, which is given as,

$$\lambda = \left(\frac{\varepsilon_{Si}\varepsilon_0 kT}{q^2 N_A}\right)^{0.5} \quad (3)$$

where, k is the Boltzmann constant, T is the absolute temperature, and N_A is the doping concentration of *p*-type Si substrate. The N_A value was calculated from the slope the $1/C^2$ vs. V graph. Using the C_{FBS} value, the C_{FB} can be obtained from the series capacitance relationship which is given

$$C_{FB} = \frac{C_i C_{FBS}}{C_i + C_{FBS}} \quad (4)$$

The V_{FB} is the voltage corresponding to the C_{FB} on the high-frequency *C-V* graphs and it was graphically determined as −0.83 and −0.4 V for HCPA and ICP-sourced ALD deposited AlN films, respectively. By substituting those values in Eq. (1), N_{eff} were found as 3.04×10^9 cm^{-2} and 3.5×10^{11} cm^{-2} for the HCPA and ICP-sourced ALD deposited AlN films, respectively. All of the calculated electrical parameters of the AlN thin films are summarized in Table 1.

Some studies related to the effective charge densities in AlN films have been reported. For example, Engelmark *et al.*[22] reported the order of 10^{12} cm^{-2} for AlN films deposited by reactive sputtering, Eom *et al.*[23] reported the order of 10^{12} cm^{-2} for AlN films deposited by sequential injection of TMA and NH_3 under UV radiation, Olivera *et al.*[24] reported the order of 10^{12} cm^{-2} for AlN films deposited by dc magnetron sputtering, Wu *et al.*[25] reported that the order of 10^{13} cm^{-2} for AlN films deposited by radio frequency magnetron sputtering, Pantojas *et al.*[8] reported that the order of 10^{11} cm^{-2} for AlN films deposited by MBE, Adam *et al.*[26] reported that the order of 10^{13} cm^{-2} for AlN films deposited by MBE reactive magnetron sputtering. The values reported in this paper (3.04×10^9 cm^{-2}) are better than in the literature for AlN thin films deposited using various methods and suggest that AlN thin films with low effective charge densities can be deposited successfully using hollow-cathode plasma sourced ALD technique.

On the other hand, the threshold onset voltage (V_{th}) was calculated for strong inversion region of the capacitor devices according to relation:

$$V_{th} = V_{FB} + 2\psi_B + \frac{(4q\varepsilon_{Si}\varepsilon_0 N_A|\psi_B|)^{1/2}}{\varepsilon_d\varepsilon_0/t_d} \quad (5)$$

where $\psi_B = (kT/q)\ln(N_A/n_i)$ and n_i is the intrinsic carrier concentration of Si at room temperature (i.e., 1.45×10^{10} cm^{-3}). Using these parameters, the threshold onset voltage (V_{th}) was obtained as −0.096 and 0.4 V for the HCP and ICP-sourced ALD deposited AlN films, respectively. Wu *et al.* reported that the threshold voltage as 10 V for (002) orien-

Table 1. Electrical parameters of the HCPA-ALD and ICP-ALD deposited AlN thin films as calculated from *C-V* curves at 1 MHz.

Plasma Source	λ-Debye l. (cm)	C_{FBS} (pF)	C_i (pF)	C_{FB} (pF)	V_{FB} (V)	ϕ_{ms} (eV)	ε_d	N_{eff} (cm^{-2})	V_{th} (V)
HCPA	1.1×10^{-5}	98	123	55	−0.83	−0.824	6.6	3.04×10^9	−0.096
ICP	8.1×10^{-6}	76	75	38	−0.4	−0.84	7.1	3.5×10^{11}	0.4

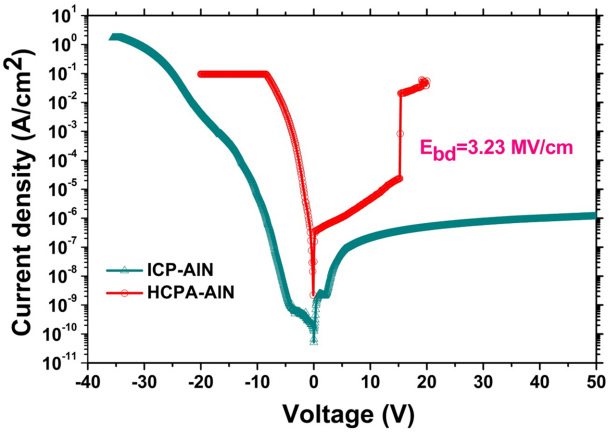

Fig. 4. *I-V* characteristics of the ICP and HCPA-deposited AlN capacitor devices.

tated AlN thin films and they attributed those high threshold voltages to many defects and vacancies in the films. Song *et al.*[27] reported that the threshold voltage as 1.103 V for ion beam enhanced deposited AlN thin films. The obtained threshold voltages and effective charge densities in this study are low compared to the reported values. This situation is may attributed to HCPA-ALD and ICP-ALD deposited AlN thin films with good crystal quality.

The leakage current density is one of the most important electrical parameters of the capacitors. As can be seen from Fig. 4, the leakage current density for the HCPA-sourced ALD deposited AlN films is higher than ICP-sourced ALD deposited AlN films. At reverse bias region of HCPA-sourced ALD deposited AlN films, the breakdown voltage is about 15.1 V and the breakdown field is calculated to be 3.23 MV/cm. But, no abrupt current increase is observed at reverse bias region of ICP-deposited AlN films, it suggests the ICP-deposited AlN films have not been broken down during the test. In other words, the breakdown voltage is larger than 50 V (exceeding the measurement range of our measurement system), and thus the breakdown field is definitely larger than 10 MV/cm that beyond the values reported in the literature for AlN films.[28-30]

In our previous studies, we reported on the electrical conduction mechanisms for ICP and HCPA-sourced ALD deposited AlN thin films. For ICP-deposited AlN films, nitrogen vacancies and N_{Al} antisite defects were related to conductivity.[16] On the other hand, in addition to nitrogen vacancies, *DX*-centers formed with the involvement of Si atoms into the AlN layers were related to conductivity for HCPA-sourced ALD deposited AlN films.[31] Most probably, these centers are caused by the Si substrate and formed near the AlN/Si interface.[32] GIXRD and ellipsometry measurements suggest that the structural quality of the HCPA-sourced ALD deposited AlN films have better and effective charge densities of those films are lower. However, lower dielectric constant, higher leakage current density, and lower breakdown field were measured for HCPA-ALD AlN films. The improvement in structural quality may be related to the higher plasma density of the HCP source. But higher plasma density causes the degradation of surface quality ($rms_{HCPA\text{-}AlN} > rms_{ICP\text{-}AlN}$), causes interface states, and our opinion these interface states play an active role in the electrical deterioration.

4. CONCLUSIONS

In this paper, polycrystalline wurtzite AlN thin films were deposited on *p*-Si substrates at 200 °C by hollow-cathode plasma and inductively coupled RF-plasma sourced atomic layer deposition technique and the effects of two different plasma sources on the electrical properties studied. Using the high frequency-*C-V* and *I-V* measurements of Al/AlN/*p*-Si MIS capacitors, we have obtained the basic electrical parameters. The effective charge density (N_{eff}) was found as 3.04×10^9 cm^{-2} for HCPA-sourced ALD deposited AlN films and this value is better than reported values in the literature. HCPA-sourced ALD deposited AlN thin films have the formation of highly oriented (002) preferential plane which indicates enhanced crystal quality, but the surface morphologies of those films were poorer. On the other hand, lower dielectric constant, higher leakage current density, and lower breakdown field were measured from HCPA-sourced ALD deposited AlN thin films. This situation was attributed to the involvement of Si atoms into the AlN layers during the HCPA-sourced ALD processing leads to additional current path at AlN/Si interface and might impair the electrical properties. These results show that although hollow-cathode plasma sourced ALD technique is one of the significant potential deposition methods to deposit AlN thin films with low effective charge densities and good crystal quality, ICP-sourced ALD technique appears to be a better than other methods to obtain good electrical characteristics.

ACKNOWLEDGMENTS

The authors would like to thank Seda Kizir and Ali Haider for AlN films deposition. This work was performed at UNAM supported by the State Planning Organization (DPT) of Turkey through the National Nanotechnology Research Center Project.

REFERENCES

1. M. S. Lee, S. Wu, S. B. Jhong, K. H. Chen, and K. T. Liu, *J. Nanomater.* **2014**, 250439-1 (2014).
2. M. S. Sun, J. C. Zhang, J. Huang, J. F. Wang, and K. Xu, *J. Cryst. Growth* **436**, 62 **(**2016).
3. H. V. Bui, F. B. Wiggers, A. Gupta, M. D. Nguyen, A. A. I.

Aarnink, M. P. de Jong, and A. Y. Kovalgin, *J. Vac. Sci. Technol. A* **33**, 01A111 (2015).
4. K. H. Chiu, J. H. Chen, H. R. Chen, and R. S. Huang, *Thin Solid Films* **515**, 4819 (2007).
5. M. Bosund, T. Sajavaara, M. Laitinen, T. Huhtio, M. Putkonen, V. M. Airaksinen, and H. Lipsanen, *Appl. Surf. Sci.* **257**, 7827 (2011).
6. M. Razeghi and R. A. McClintock, *J. Cryst. Growth* **311**, 3067 (2009).
7. T. V. Blank and Y. A. Gol'dberg, *Semiconductors* **37**, 1000 (2003).
8. C. R. Ortiz, V. M. Pantojas, and W. O. Rivera, *Solid State Electron.* **91**, 106 (2014).
9. B. Abdallah, S. Al-Khawaja, A. Alkhawwam, and I. M. Ismail, *Thin Solid Films* **562**, 152 (2014).
10. B. Abdallah, S. Al-Khawaja, and A. Alkhawwam, *Appl. Surf. Sci.* **258**, 419 (2011).
11. A. M. Ivanov, I. M. Kotina, M. S. Lasakov, N. B. Strokan, and L. M. Tuhkonen, *Semiconductors* **44**, 1031 (2010).
12. Y. Tanaka, Y. Hasebe, T. Inushima, A. Sandhu, and S. Ohoya, *J. Cryst. Growth* **209**, 410 (2000).
13. F. Jose, R. Ramaseshan, S. Dash, S. Bera, A. K. Tyagi, and B. Raj, *J. Phys. D Appl. Phys.* **43**, 075304 (2010).
14. M. Leskela, J. Niinisto, and M. Ritala, *Comph. Mater. Process.* **4**, 101 (2014).
15. M. Ritala, M. Leskelä, E. Nykänen, P. Soininen, and L. Niinistö, *Thin Solid Films* **225**, 288 (1993).
16. H. Altuntas, C. Ozgit-Akgun, I. Donmez, and N. Biyikli, *IEEE Trans. Electron Dev.* **62**, 3627 (2015).
17. H. Altuntas, C. Ozgit-Akgun, I. Donmez, and N. Biyikli, *J. Appl. Phys.* **117**, 155101 (2015).
18. H. C. Barshilia, B. Deepthi, and K. S. Rajam, *Thin Solid Films* **516**, 4168 (2008).
19. C. Ozgit-Akgun, E. Goldenberg, A. K. Okyay, and N. Biyikli, *J. Mater. Chems. C*, **2**, 2123 (2014).
20. Z. X. Bi, Y. D. Zheng, R. Zhang, S. L. Gu, Q. Xiu, L. L. Zhou, B. Shen, D. J. Chen, and Y. Shi, *J. Mater. Sci. Mater. El.* **15**, 317 (2004).
21. X. H. Xu, C. J. Zhang, and Z. H. Jin, *Thin Solid Films* **388**, 62 (2001).
22. F. Engelmark, J. Westlinder, G. F. Iriarte, I. V. Katardjiev, and J. Olsson, *IEEE Trans. Electron. Dev.* **50**, 1214 (2003).
23. D. Eom, S. Y. No, C. S. Hwang, and H. J. Kim, *J. Electrochem. Soc.* **153**, C229 (2006).
24. I. C. Oliveira, M. Massi, S. G. Santos, C. Otani, H. S. Maciel, and R. D. Mansano, *Diam. Relat. Mater.* **10**, 1317 (2001).
25. C. I. Wu and A. Kahn, *Appl. Phys. Lett*. **74**, 546 (1999).
26. T. Adam, J. Kolodzey, C. P. Swann, M. W. Tsao, and J. F. Rabolt, *Appl. Surf. Sci.* **175-176**, 428 (2001).
27. Z. R. Song, Y. H. Yu, D. S. Shen, S. C. Zou, Z. H. Zheng, E. Z. Luo, and Z. Xie, *Mater. Lett.* **57**, 4643 (2003).
28. K. Tsubouchi and N. Mikoshiba, *IEEE Trans. Sonics Ultrason*. **32**, 634 (1985).
29. E. V. Gerova, N. A. Ivanov, and K. I. Kirov, *Thin Solid Films* **81**, 201 (1981).
30. A. Fathimulla and A. A. Lakhani, *J. Appl. Phys*. **54**, 4586 (1983).
31. H. Altuntas, T. Bayrak, S. Kizir, A. Haider, and N. Biyikli, *Semic. Sci. Tech*. **31**, 075003 (2016).
32. V. Ligatchev, Rusli, and Z. Pan, *Appl. Phys. Lett*. **87**, 242903 (2005).